MDCK Cell Cultures as an Epithelial *In Vitro* Model: Cytoskeleton and Tight Junctions as Indicators for the Definition of Age-Related Stages by Confocal Microscopy

Barbara Rothen-Rutishauser,[1,3] Stefanie D. Krämer,[2] Annette Braun,[1] Maja Günthert,[1] and Heidi Wunderli-Allenspach[1]

Received December 23, 1997; accepted April 14, 1998

Purpose. Madin Darby Canine Kidney (MDCK) cells were grown in culture, and age-related morphological changes in the cytoskeleton and tight junction (TJ) network were used to define stages in view of establishing an optimal *in vitro* model for the epithelial barrier.

Methods. Growth curves and transepithelial electrical resistance (TEER) were determined, and the cytoskeleton (actin, α-tubulin, vimentin) and TJ (Zonula occludens proteins ZO1, ZO2) were investigated with immunofluorescent methods by confocal laser scanning microscopy (CLSM) and digital image restoration.

Results. TEER measurements indicated that TJ were functional after one day. Values then remained constant. Four morphological stages could be distinguished. Stage I (0–1 day): Sub confluent cultures with flat cells; TJ established after cell-to-cell contacts are made. Stage II (2–6 days): Confluent monolayers with a complete TJ network, which remains intact throughout the later stages. Stage III (7–14 days): Rearrangement in the cytoskeleton; constant cell number; volume and surface area of cells reduced (cobble-stone appearance). Stage IV (≥ 15 days): Dome formation, i.e. thickening and spontaneous uplifting of the cell monolayer.

Conclusions. Based on the structural characteristics of stage III cell cultures, which are closest to the *in vivo* situation, we expect them to represent an optimal *in vitro* model to study drug transport and/or interactions with drugs and excipients.

KEY WORDS: MDCK cells; confocal laser scanning microscopy; cytoskeleton; tight junctions; *in vitro* epithelial cell model; age-related changes.

INTRODUCTION

The limiting factor for the successful therapeutic application of new drugs is very often their transport into the system (1). There is a great need for standardised *in vitro* models, which permit an early and easy screening for the permeation characteristics of large numbers of molecules (2). Madin Darby Canine Kidney (MDCK) cells are among the best studied epithelia. This cell line has been well characterised regarding morphology, electrical resistance, respective composition of the apical and basolateral cell membranes and other factors (review see (3)). This provides an excellent basis for their use as standardised *in vitro* model for drug transport and interaction studies with drugs and excipients. During formation of polarised monolayers of MDCK cells, tight junctions (TJ) are established as soon as cell-to-cell contacts are made. They move upward from the site of cell-substratum contact to a lateral position and form a gasket-like seal which prevents free diffusion of solutes from the lumen to the interstitium (for review see (4)). After remodelling of the cytoarchitecture the microtubules are organised in an apical web and longitudinal microtubule bundles in the apical-basal axis of the columnar cells (5). Actin is localised along the lateral walls in addition to stress fibres which traverse the basal parts of polarised cells (6). It has been suggested that the actin cytoskeleton, which is anchored to the cell membrane through the adherens junctions, plays a role in the formation and maintenance of TJ. Evidence comes from the fact that the formation of TJ in epithelial cells depends on the prior formation of E-cadherin mediated adherens junctions (7,8). After trypsinisation of confluent MDCK cell cultures and reseeding at high cell density, attachment and reformation of cell contacts are synchronous. MDCK cells thus also provide an excellent model to study the formation of TJ and their function *in vitro* (9).

For morphological studies confocal laser scanning microscopy (CLSM) has emerged as the best solution to provide images in which out-of-focus blur is essentially absent. The major advantage over conventional optical microscopy is a significant improvement in axial (z) and also in lateral resolution, if the confocal pinhole is sufficiently small. Direct non-invasive serial optical sectioning of intact and even living cells in combination with digital image processing produces a superior visual quality (10,11). Layers up to about 150 μm thickness can be studied. The CLSM technique is particularly suited for studies with thick cell layers, which are more closely related to the *in vivo* situation than the often used "just confluent," flat monolayers. Optimal results are obtained with the simultaneous use of several fluorescent markers for cellular components like nuclei and cytoskeleton, which permit easy orientation within the cell layers.

In the present work age-related changes in MDCK cell cultures are described. Growth curves were established and the TEER was measured. The remodelling of the cytoskeleton and the organisation of the TJ were studied with immunofluorescent methods in combination with CLSM. This approach allowed to define four age-related stages (I to IV) which will be discussed in view of their qualities as an *in vitro* epithelial cell model.

MATERIALS AND METHODS

Cell Culture. MDCK cells (passage 202) were a gift from Michel Paccaud (Institut d'Hygiène, Geneva, Switzerland). Cells were used between passage 216 and 270. Doubling times determined around passage 210 and at regular intervals thereafter were stable at about 20 hours (representative growth curve see Results, Fig. 1). Cultures were regularly tested for mycoplasm infections. Monolayers were propagated on plastic TPP®-flasks (Winiger AG, Wohlen, Switzerland) in Eagle's minimum essential medium (MEM) with Earl's salts supple-

[1] Biopharmacy, Department of Pharmacy, ETH Zürich, CH-8057 Zürich, Switzerland.

[2] Sanofi Recherche, F-34184 Montpellier, France.

[3] To whom correspondence should be addressed. (e-mail: brothen@pharma.ethz.ch)

ABBREVIATIONS: CLSM, confocal laser scanning microscopy; MDCK, Madin Darby Canine Kidney; TEER, transepithelial electrical resistance; TJ, tight junction(s); ZO, zonula occludens.

0724-8741/98/0700-0964$15.00/0

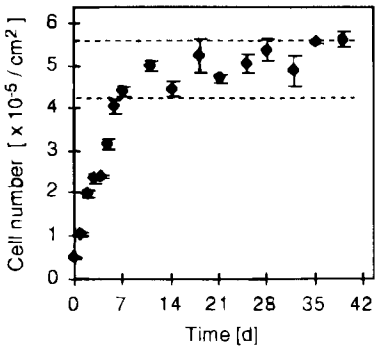

Fig. 1. Representative growth curve of MDCK cell cultures. Cells (passage 228) were cultivated on 6-well plates under standard conditions and counted at various times. Each point represents the mean ± standard deviation of 3 individual culture wells.

mented with 20 mM HEPES (ICN Biomedicals Inc.) and 10% foetal calf serum. Incubations were in a 5% CO_2 atmosphere at 37°C. To establish growth curves cells were propagated in TPP® 6-well plates. Cell numbers were determined with a Neubauer counting chamber. Experimental cultures were grown on Falcon® Cell Culture Inserts with a Cyclopore® membrane (0.4 μm #3090; Becton Dickinson) with 2.5 ml medium in the upper, and 3 ml in the lower chamber. Confluence was reached at the same time as with cultures grown on 6-well plates. For long-term cultures medium was changed twice weekly, and fresh medium was added routinely 24 hours before an experiment was performed. Electrical resistance was measured with the Millicell-ERS system (MERS 000 01, Millipore). The electrical resistance of filters without cells was subtracted from all samples. Resistance values were multiplied with the surface area of the inserts (4.2 cm^2).

Antibodies and Fluorescent Reagents. The anti ZO1 monoclonal antibody and the affinity purified secondary antibodies (IgG) conjugated with cyanine 5 or 3 were purchased from Chemicon. The anti α-tubulin (Clone DM 1A) and the anti vimentin cyanine 3-conjugated antibody (Clone C-9080) were purchased from Sigma, fluorescein phalloidin from Molecular Probes. The anti ZO2 antiserum was a kind gift of Daniel A. Goodenough, Harvard Medical School, Boston, MA. Cell nuclei were visualised with 4,6-Diamidino-2-Phenylindole (DAPI) from Hoechst (#333342). The specificity of the antibodies and the labeling procedure was tested with the following control experiments: use of secondary antibodies only, and parallel use of two types of labelled secondary antibodies differing in the wavelength of the coupled fluorochrome. All antibodies were highly specific.

Immunofluorescent Labeling. Membranes with cell layers were washed in PBS (10 mM phosphate buffered saline pH 7.4: 130 mM NaCl, Na_2HPO_4, KH_2PO_4) and fixed for 15 min at room temperature in 3% paraformaldehyde in PBS. Fixed cells were treated with 0.1 M glycine in PBS for 5 min, permeabilised in 0.2% Triton X-100 in PBS for 15 min. Samples were incubated at 37°C with the first antibody for 60 min and with the second antibody for 90 min. Antibodies were diluted in PBS containing 3% bovine serum albumin: anti ZO1 1:100, anti ZO2 1:500, anti α-tubulin 1:500, anti vimentin 1:50. Anti rabbit cyanine 5 and anti rat cyanine 3 were both diluted 1:50. The dilution for fluorescein phalloidin was 1:10 and for the DAPI stain 1:100. Preparations were mounted as described (12). To preserve the structural organisation of microtubules a special microtubule protective buffer pH 6.9 (MP-buffer) was used: 65 mM PIPES, 25 mM HEPES, 10 mM EGTA, 3 mM $MgCl_2$ (13). Cells were permeabilised for 1 min in 1% Triton X-100 in MP-buffer and then fixed for 10 min in 3% PFA/MP-buffer. For antibody labeling the same procedure was used as described above.

Confocal Microscopy. A Zeiss LSM 410 inverted microscope was used (lasers: HeNe 633 nm, HeNe 543 nm, Ar 488/514 nm and Ar UV 364 nm). Up to three fluorochromes could be scanned simultaneously. Optical sections at intervals of 0.25 μm were taken with a 63×/1.4 Plan-Apochromat objective. Image processing was done on a Silicon Graphics workstation using IMARIS, a 3D multi-channel image processing software for confocal microscopic images (Bitplane AG, Zurich, Switzerland).

RESULTS

Age-Related Growth Characteristics of MDCK Cells

Growth curves were established under standard conditions (Materials and Methods). MDCK cells seeded at a density of 5×10^4 cells/cm^2 grew confluent within 2 days. The cell number reached a plateau of 4.2 to 5.7 $\times$ 10^5 cells/cm^2 after 7 days and remained in the stationary phase at least for 35 days (Fig. 1). TEER measurements were performed at various times after seeding. The highest value of about 550 Ωcm^2 was obtained after 18 hours. It decreased to about 250 Ωcm^2 during the next 30 hours and then remained stable between 180 and 250 Ωcm^2 (Fig. 2).

Age-Related Changes as Observed by CLSM

MDCK cells were grown under standard conditions and prepared for CLSM microscopy at various time points. They

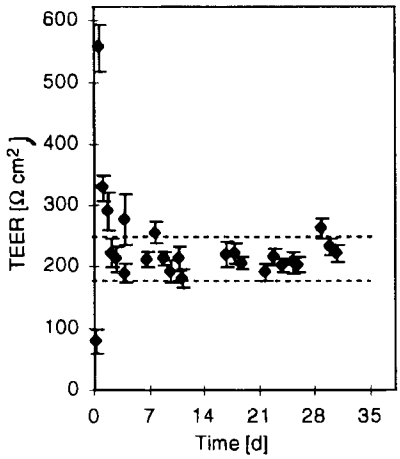

Fig. 2. Time-dependent development of TEER across MDCK cell monolayers. Representative curve with cells from passage 228 cultivated on inserts under standard conditions. TEER measurements were performed at various times after seeding. Each point represents the mean ± standard deviation from 3 inserts (6 measurements per insert).

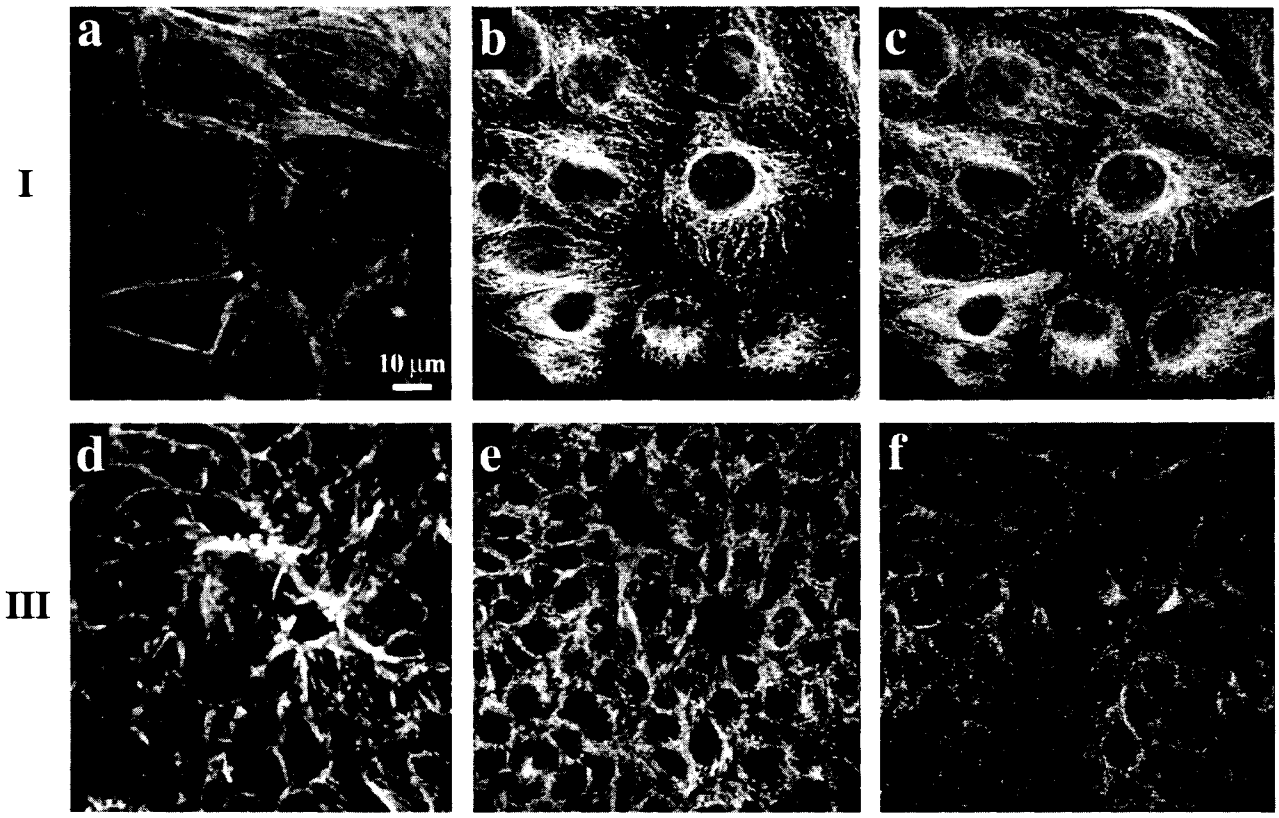

Fig. 3. The cytoskeleton of MDCK cells in culture. MDCK cells were grown under standard conditions on cell culture inserts and prepared for CLSM: (stage I) after 1 day (a, b, c), and (stage III) after 11 days (d, e, f). The cells were triple-stained for F-actin (a, d), α-tubulin (b, e), and vimentin (c, f). All pictures are single optical sections taken close to the membrane filter.

were labeled with various markers as described in Materials and Methods. Significant age-related changes in MDCK cell cultures were observed whereby four morphologically distinct stages (I to IV) could be defined.

Cytoskeletal Organization

Stage I (0 to 1 day). One day after seeding the cells were not yet confluent. They contained long actin filaments (Figs. 3a, 4a). The microtubules were found in the perinuclear area and throughout the cytoplasm as a thin network (Figs. 3b, 4b). For the intermediate filaments a similar distribution was observed as for the microtubules (Fig. 3c). The projection of a confocal data set of cells triple-stained for actin, α-tubulin and the cell nuclei (Fig. 4c) shows that MDCK cell monolayers are very flat (2 to 3 µm) with a diameter of 20 to 30 µm and an average cell volume of about 2700 μm^3 (Table 1).

Stage II (2 to 6 days). Although the cells had grown confluent after 2 days, cell numbers continued to increase exponentially (see Fig. 1). In MDCK cells cultured for 4 days actin was preferentially localised at the cell border and in stress fibres which traverse the basal parts of polarised cells (Fig. 4d). α-tubulin was very dense around the cell nuclei (Fig. 4e). Vimentin showed a similar distribution as α-tubulin (data not shown). The thickness of the monolayers had increased to 6 to 8 µm (Fig. 4f), whereas the average cell diameter decreased to 10 to 15 µm and the average cell volume to about 1700 μm^3 (Table I).

Stage III (7 to 14 days). After 7 days in culture no further increase in cell number was observed. Cells formed monolayers with the actin arranged at the cell borders and in stress fibres close to the basal cell membrane (Figs. 3d, 4g). Staining for microtubules (Figs. 3e, 4h) and intermediate filaments (Fig. 3f)

Fig. 4. (*opposite*) Age-related changes of MDCK cell morphology. MDCK cells were grown under standard conditions on cell culture inserts and prepared for CLSM: (stage I) after 1 day (a, b, c); (stage II) after 4 days (d, e, f); (stage III) after 11 days (g, h, i), and (stage IV) after 27 days (j, k, l). Cells were double-stained for F-actin (a, d, g, j), and α-tubulin (b, e, h, k), or triple-stained (c, f, i, l) for F-actin (green), α-tubulin (red) and cell nuclei (blue). The same data sets are shown in (a, b), (d, e), (g, h) and (j, k), respectively. Pictures a, b, d, e, g, h, j, k are single optical sections taken close to the membrane filter. Pictures c, f, i, l represent xy-projections, pictures c′, f′, i′, l′ represent xz-projections, and pictures c″, f″, i″, l″ represent yz-projections. The arrows in i′, i″ and l′ point to the surface protrusions which are positive for α-tubulin. The arrowhead in l″ indicates that the microtubules in a dome are concentrated at the apical surface of the cell layer. The asterisks in Fig. 4k represent a cut through a dome where the microtubules were on a different layer.

Table I. Characteristics of Stages I to IV

Time after seeding [days]	Cell number [$\times 10^{-5}$/cm^2]	TEER [Ω cm^2]	Cell layer thickness [μm][a]	Cell diameter [μm][a]	Cell volume [μm^3][b]	Remarks
1 (stage I)	1.05 ± 0.04	330 ± 20	2–3	20–30	1312–4050	Subconfluent cultures, flat cells, high TEER
4 (stage II)	2.37 ± 0.06	190 ± 16	6–8	10–15	1020–2336	Confluent cultures, complete network of TJ, constant TEER range
11 (stage III)	4.98 ± 0.13	182 ± 16	6–8	8–10	573–959	Confluent cultures (stationary phase), complete network of TJ, polarisation into apical and basolateral domains, constant TEER range
27 (stage IV)	5.37 ± 0.27	265 ± 40	6–8 (m)[c] 15–30 (d)	8–10 (m) 8–10 (d)	743–963 (m) 1045–1627 (d)	As stage III, and in addition formation of domes

[a] Measurements were performed with the IMARIS software (Material and Methods). Values are from 10–12 cells.
[b] Average cell volumes were estimated from fluorescein phalloidin labeled cells scanned with a step size of 0.25 μm and analysed with the Depth Analyse program, which is part of the IMARIS software.
[c] (m) MDCK cell monolayer; (d) MDCK domes.

was very strong around the nuclei and throughout the cytoplasm. Cell monolayers were about 6 to 8 μm thick and had assumed a cobble-stone appearance (Fig. 4i). Protrusions on the cell surface could be observed, usually 1 per cell, which were positive for α-tubulin (Fig. 4i′,i″, arrows) and vimentin (not shown) but excluded filamentous actin. The cell diameter was reduced to 8 to 10 μm, the average volume to about 770 μm^3 (Table I).

Stage IV (≥15 days). Actin was found along the lateral walls (Fig. 4j), and in the form of stress fibres traversing the basal parts of cells (Fig. 4l). The staining for microtubules (Fig. 4k) and intermediate filaments (not shown) was very strong around the nuclei and throughout the cytosplasm. Around day 15 the cell layer began to develop small elevations and within the next days dome formation was observed (Fig. 4l) as previously described (14). These domes, consisting of monolayers, are clearly visible in xz- and yz-projections (Fig. 4l′, 4l″). The heights of the domes varied from 15 to 30 μm. Within the domes the microtubules were concentrated near the apical membranes (Fig. 4l″, arrowhead). Fig. 4k shows a single optical section taken close to the filter membrane. α-tubulin positive protrusions were present at the apical surface (Fig. 4l′, arrow). In contrast, vimentin was localised throughout the cytoplasm (not shown). Thickness, diameter and the average volume of cells in the monolayer remained constant as compared to stage III, however, the average volume of cells in the domes had increased to about 1300 μm^3 since their height increased from 6–8 μm to 15–30 μm (Table I).

Organization of Tight Junctions

Stage I (0 to 1 day). Triple-stains with fluorescein phalloidin and antibodies against ZO1 and ZO2 provided interesting insights to the formation of TJ. Fig. 5 focuses on an area where cell-cell contacts are seen at various stages. Actin clearly marked the border of the cells (Fig. 5b, arrow) but was also distributed throughout the cytoplasm (Fig. 5b). The TJ proteins ZO1 and ZO2 lined the cell-cell contacts (Fig. 5a, c, arrows). ZO2 but not ZO1 was also found within the cytoplasm. At sites with no cell-cell contacts (Fig. 5, asterisks) neither ZO1 nor ZO2 were found along the cell borders. The arrowheads point to an area where the formation of a TJ is "frozen" in a stage, in which actin formed a solid line along the cells which established a contact, whereas ZO2 and ZO1 appeared only at the direct contact site. ZO1 is less prominent than the other two and shows up as a dotted rather than a solid line.

Stage II (2 to 6 days). The localisation of ZO1 is shown together with the actin cytoskeleton and the cell nuclei in a projection (Fig. 5d) and a 3D reconstruction (Fig. 5e) of the same confocal data set. ZO1 was associated exclusively with TJ at the apical side of the cells (Fig. 5d′, d″, arrows). No

Fig. 5. (*opposite*) Tight junctions in MDCK cells in culture. MDCK cells were grown under standard conditions on cell culture inserts and prepared for CLSM: (stage I) after 1 day (a, b, c); (stage II) after 4 days (d, e, f); (stage III) after 11 days (g, h, i), and (stage IV) after 27 days (j, k, l). Pictures a, b, c show the same data set of cells which were triple-stained for ZO1 (a), F-actin (b), and ZO2 (c). The arrows point to an established TJ between neighbouring cells. The arrowheads point to a cell-cell contact which is "frozen" in formation. The asterisks indicate cell borders without cell-cell contact, where only actin, but neither ZO1 nor ZO2 appear. Pictures d, e, g, h, j, k illustrate triple-stained preparations: F-actin (green), ZO1 (red) and cell nuclei (blue). The same data sets are shown in (d, e), (g, h) and (j, k) respectively. The arrows in d′, d″ and j′, j″ point to TJ which are localised near the apical surface and the asterisks point to dividing cells. Pictures f, i, l show cells stained for ZO2. a, b, c, e, f, h, i, k, l are 3D reconstructions. d, g, j represent xy-projections, d′, g′, j′ represent xz-projections, and d″, g″, j″ represent yz-projections.

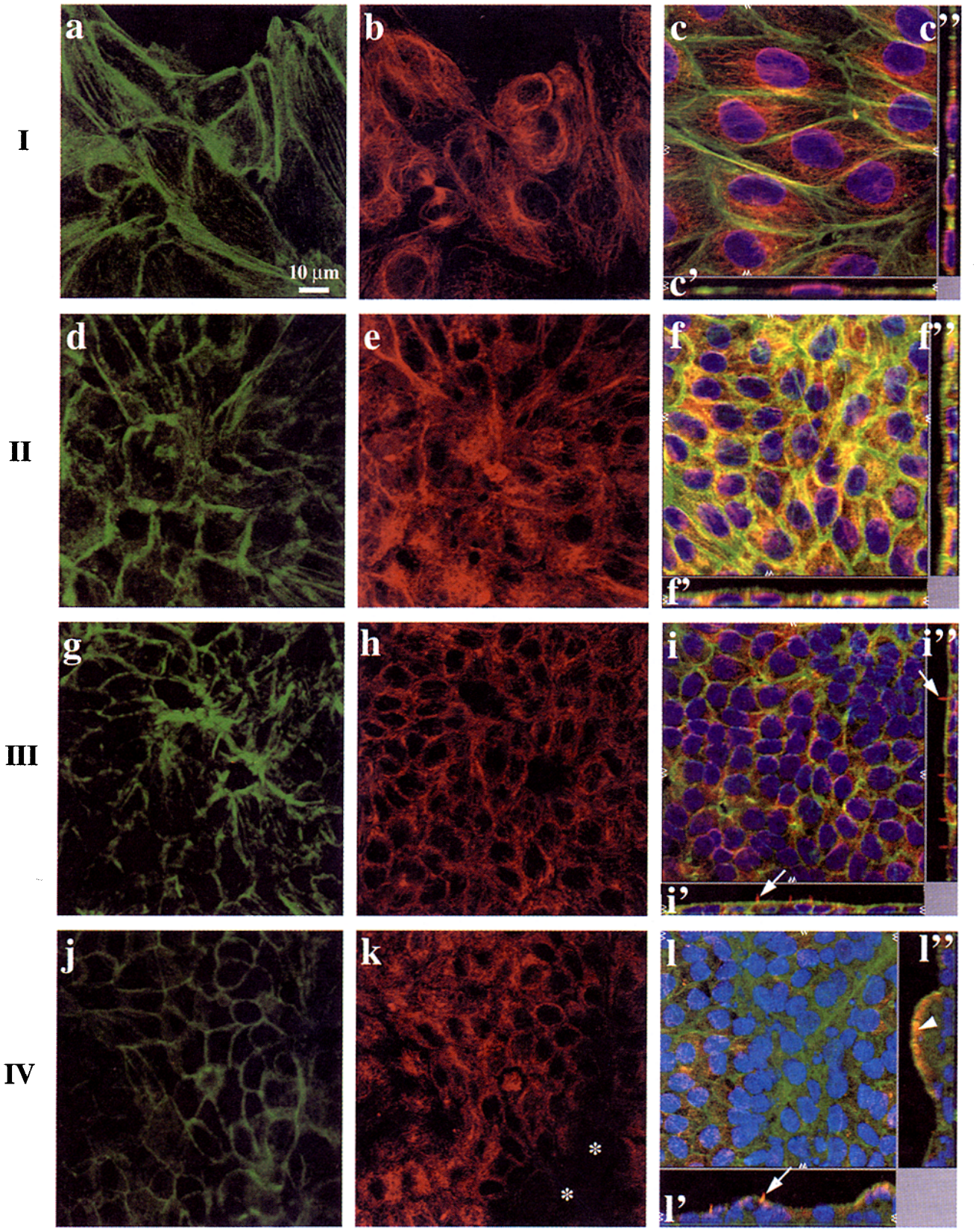
I
II
III
IV
a
b
c
c''
c'
10 µm
d
e
f
f''
f'
g
h
i
i''
i'
j
k
l
l''
l'

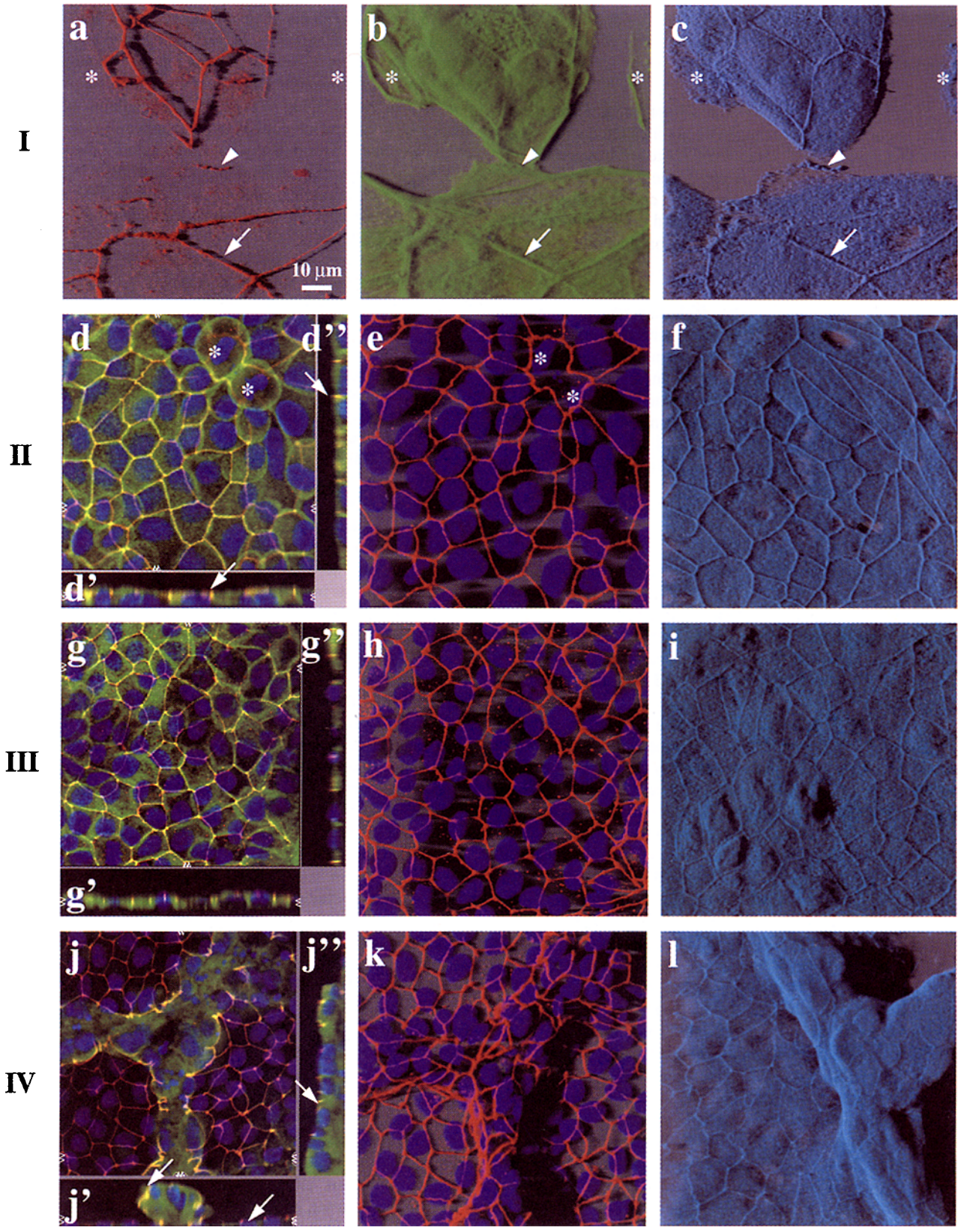
I
II
III
IV
a
b
c
d
d''
d'
e
f
g
g''
g'
h
i
j
j''
j'
k
l
10 µm

functional TJ were present between dividing cells (Fig. 5d, e, asterisks). ZO2 was found along the outlines of the cells and throughout the cytoplasm (Fig. 5f).

Stage III (7 to 14 days). The TJ appear as a continuous network between neighbouring cells. As illustrated with the xz- and yz-projections (Fig. 5g) and the 3D reconstruction of ZO1 and the cell nuclei (Fig. 5h), the TJ network was localised close to the apical cell surface separating apical and basolateral domains. ZO2 was localised at the TJ and throughout the cytoplasm (Fig. 5i) as well as along the basolateral membrane (not shown).

Stage IV (≥15 days). The ZO1 network was localised close to the cell surface both in areas with flat, cobble-stone-like monolayers (Fig. 5j′, arrow) and in domes (Fig. 5j′, j″, arrows). The 3D reconstruction of ZO1 and the cell nuclei (Fig. 5k) clearly shows the continuous TJ network. The shadow resulting from the uplifted cell layer (dome) is artificially cast in this picture (SFP mode of the IMARIS software); it partially hides the TJ network. ZO2 was localised along the cell borders and in the cytoplasm (Fig. 5l).

DISCUSSION

The characterisation of MDCK long-term cultures using a combined approach of CLSM, growth curves and TEER measurements has provided important information on the development of the polarised epithelial cell monolayers. As we could show no synchrony exists between cell numbers, the development of TEER, the establishment of TJ and the cytoskeletal organisation.

A peak in TEER was reached at a time when cells had not yet grown confluent. TEER values then dropped to a lower level which remained constant from day 2 to at least day 30. The initial peak followed by a marked drop has previously been observed in MDCK monolayers (15) and in MDCK cells after restoration of Ca^{2+} (9). It was attributed to a difference in the time course of junctional sealing and installation of channels in the TJ. The plateau of about 180 to 250 Ωcm^2 reached after 2 days corresponds very well to the range found after 3 to 4 days (earlier time points are not available) for the ATCC strain used by Cho *et al.* (16), i.e., the MDCK cells used in this study represent a type II (low resistance) strain. It is interesting to note that the TEER is not changing significantly at the time when constant cell numbers are reached, and also the remodelling of the cytoskeleton, which results in a thickening of the cell layer and finally in dome formation, is not reflected in a change in TEER. This long-term time course of the TEER was reproducibly observed when cells were grown under our standard conditions, which comprise a constant seeding density of 5×10^4 cells/cm^2. In this context it is important to note that variations in the seeding density of cells and in the underlying substratum can also influence the TEER (17).

An important parameter for the definition of age-related stages in long-term MDCK cultures was the cytoarchitecture. As could be demonstrated with phalloidin labeling of the filamentous actin molecules, rearrangements took place not only in the early stages up to confluence. Significant changes were found as soon as cell numbers reached a plateau, i.e. after about 7 days, and again when dome formation started, i.e. around day 15. Rearrangements were not only found with actin, but also with α-tubulin and vimentin, which both have a very similar distribution pattern. The remodelling of the cytoarchitecture could best be followed in axial optical sections, i.e. in the xz- and yz-projections. Only in stage III the regular cobble-stone arrangement typical of epithelial cells appears. Our findings are in agreement with recently published data on the detergent solubility of structural proteins in long-term MDCK cell cultures (18). The decreasing solubility in Triton X-100 goes parallel with the compact cobble-stone appearance of cells and the formation of domes.

An interesting feature was detected when the cytoskeletal markers were used for labeling in stage III. At this stage cells became decorated with protrusions (~1 per cell, about 2–3 μm long), which contain α-tubulin and vimentin, but no filamentous actin. These structures persist when domes are formed, i.e. when thickening and uplifting of the monolayer occurs. Their function is hitherto unknown. They most probably correspond to the previously described cilia (19).

The TJ network, which plays an important role as a gasket-like seal for the epithelial layer (20,4), is formed already during stage 1. Although time-sequence experiments with living cells have not yet been performed there is evidence that upon formation of TJ not all TJ proteins appear at the same time. The triple stained preparation illustrated in Fig. 5a, b, c allows to hypothesise about the formation of TJ. Actin is present in the cytoplasm and at the borders of growing cells already before they make contact with other cells. ZO2 is also present in the cytoplasm (21), however, it only appears at the membrane if a cell-cell contact has been established. ZO1 is not found in the cytoplasm but exclusively at the membrane in the TJ area. It is striking to note that of the three proteins actin first seems to form a tight contact between two neighbouring cells resulting in a solid line. In contrast ZO2 and even more so ZO1 initially appear like pearls on a string before they organise into solid lines as well. To get more information on the kinetics of TJ formation, in particular on the role of ZO1, the localisation of ZO1 in living cells is presently being studied with a chimerical protein between ZO1 and green fluorescent protein (GFP). Once confluent monolayers are formed and cell-cell contacts established, a complete network of TJ is present. The cells begin to reorganise their cytoarchitecture, which results in the functional polarisation of the cells, and in this process the TJ move towards the apical side as already described previously (5). The TJ network remains intact throughout the later stages. This can readily be followed with the SFP, a shadow projection mode of the IMARIS software program, used in Fig. 5e, h, k. TJ stay close to the apical side also after domes are formed as can best be seen in the axial projections (Fig. 5d, g, j). *In vitro* most epithelia other than the MDCK cells and most endothelial cells do not have a continuous network of TJ under standard culture conditions although the TJ proteins are expressed (Rothen-Rutishauser, unpublished). The fact that a complete TJ network is established and maintained in MDCK cells makes this cell line a prime candidate as a model for simple epithelia.

It is well known that various factors like growth medium, seeding density, temperature, type and concentration of serum as well as the substratum have been described to influence

growth and appearance of MDCK cells (17,22,23). In view of the use of MDCK cell cultures as an *in vitro* model, the issue of both reproducibility and variability is utterly important. The four stages defined here represent age-related changes which reproducibly occur under strictly controlled conditions. Similar age-related cytoskeletal rearrangements have been found in the meantime, for instance in Caco-2 cells (Rothen-Rutishauser, unpublished). MDCK cells have previously been used for transport studies (16). Cultures were then seeded at variable cell densities between 5×10^4 cells/cm^2 (our standard conditions) and ten times less. Experiments were performed immediately after cells were confluent, usually after 5 days. At this stage though the TEER is constant, cultures are still growing exponentially and undergo rearrangement of the cytoskeleton. This may explain that the largest differences were found between individual cell layer preparations, whereas the transport of all markers tested by Cho *et al.* (16) was independent of temperature, strain type, and TEER values.

Although the potential of CLSM has long been recognised, too many studies are still restricted to single markers. The present work illustrates that a combination of markers, e.g., for nuclei, the cytoskeleton and TJ, permits to define stages in the development of the cell cultures. In the future transport experiments can thus be combined with studies on the influence of the transported solute themselves or excipients on the cells. The transport characteristics of the stages II, III and IV will be explored and compared. Another important aspect is the susceptibility of TJ in the four stages towards permeation enhancers like EDTA, EGTA and oleic acid which is under study in our laboratory.

REFERENCES

1. K. L. Audus, R. L. Bartel, I. J. Hidalgo, and R. T. Borchardt. The use of cultured epithelial and endothelial cells for drug transport and metabolism studies. *Pharm. Res.* **7**:435–451 (1990).
2. P. Artursson and R. T. Borchardt. Intestinal drug absorption and metabolism in cell cultures: Caco-2 and beyond. *Pharm. Res.* **14**:1655–1658 (1997).
3. J. A. McRoberts, M. Taub, and M. H. Saier. The Madin Darby canine kidney (MDCK) cell line. In G. Sato (ed.), *Functionally Differentiated Cell Lines*, Alan R. Liss, Inc., New York, 1981, pp. 117–139.
4. B. Gumbiner. Structure, biochemistry, and assembly of epithelial tight junctions. *Am. J. Physiol.* **253**:749–758 (1987).
5. R. Bacallao, C. Antony, C. Dotti, E. Karsenti, E. H. K. Stelzer, and K. Simons. The subcellular organization of Madin Darby canine kidney cells during the formation of a polarized epithelium. *J. Cell Biol.* **109**:2817–2832 (1989).
6. S. Eskelinen, V. Huotari, R. Sormunen, R. Palovuori, J. W. Kok, and V.-P. Lehto. Low intracellular pH induces redistribution of fodrin and instabilization of lateral walls in MDCK cells. *J. Cell. Physiol.* **150**:122–133 (1992).
7. B. Gumbiner and K. Simons. A functional assay for proteins involved in establishing an epithelial occluding barrier: identification of a uvomorulin-like polypeptide. *J. Cell Biol.* **102**:457–468 (1986).
8. B. Gumbiner, B. Stevenson, and A. Grimaldi. The role of the cell adhesion molecule uvomorulin in the formation and maintenance of the epithelial junctional complex. *J. Cell Biol.* **107**:1575–1587 (1988).
9. L. Gonzalez-Mariscal, B. Chávez de Ramirez, and M. Cereijido. Tight junction formation in cultured epithelial cells (MDCK). *J. Membr. Biol.* **86**:113–125 (1985).
10. D. Shotton and N. White. Confocal scanning microscopy: three-dimensional biological imaging. *Trends Biochem. Sci.* **14**:435–439 (1989).
11. R. C. Gonzalez and P. Wintz. *Digital Image Processing*, Addison-Wesley Publishing Company, Reading, 1987.
12. B. M. Rothen-Rutishauser, E. Ehler, E. Perriard, J. M. Messerli, and J.-C. Perriard. Different behaviour of the non-sarcomeric cytoskeleton in neonatal and adult rat cardiomyocytes. *J. Mol. Cell. Cardiol.* **30**:19–31 (1998).
13. M. Schliwa, J. van Blerkom, and K. R. Porter. Stabilization of the cytoplasmic ground substance in detergent-opened cells and a structural and biochemical analysis of its composition. *Proc. Natl. Acad. Sci. USA* **78**:4329–4333 (1981).
14. J. E. Lever. Inducers of mammalian cell differentiation stimulate dome formation in a differentiated kidney epithelial cell line (MDCK). *Proc. Natl. Acad. Sci. USA* **76**:1323–1327 (1979).
15. M. Cereijido, E. S. Robbins, W. J. Dolan, C. A. Rutunno, and D. D. Sabatini. Polarized monolayers formed by epithelial cells on a permeable and translucent support. *J. Cell Biol.* **77**:853–880 (1978).
16. M. J. Cho, D. P. Thompson, C. T. Cramer, T. J. Vidmar, and J. F. Scieszka. The Madin Darby canine kidney (MDCK) epithelial cell monolayer as a model cellular transport barrier. *Pharm. Res.* **6**:71–77 (1989)
17. C. Butor and J. Davoust. Apical to basolateral surface area ratio and polarity of MDCK cells grown on different supports. *Exp. Cell Res.* **203**:115–127 (1992).
18. F. Cao and J. M. Burke. Protein insolubility and late-stage morphogenesis on long-term postconfluent cultures of MDCK epithelial cells. *Biochem. Biophys. Res. Comm.* **234**:719–728 (1997).
19. J. D. Valentich. Morphological similarities between the dog kidney cell line MDCK and the mammalian cortical collecting tubule. *Ann. N. Y. Acad. Sci.* **372**:384–405 (1981).
20. M. G. Farquhar and G. E. Palade. Junctional complexes in various epithelia. *J. Cell Biol.* **17**:375–412 (1963).
21. L. A. Jesaitis and D. A. Goodenough. Molecular characterization and tissue distribution of ZO-2, a tight junction protein homologous to ZO-1 and the Drosophila discs-large tumor supressor protein. *J. Cell Biol.* **124**:949–961 (1994).
22. J. E. Lever. Variant (MDCK) kidney epithelial cells altered in response to inducers of dome formation and differentiation. *J. Cell Physiol.* **122**:45–52 (1985).
23. M. M. Jaeger, V. Dodane, and B. Kachar. Modulation of tight junction morphology and permeability by an epithelial factor. *J. Membr. Biol.* **139**:41–48 (1994).